

CHAPTER IV
CARBON BLACK NANOPARTICLE-FILLED ELECTROSPUN POLY(VINYL ALCOHOL) NANOFIBERS AND THEIR MECHANICAL AND ELECTORRHEOLOGICAL PROPERTIES

4.1 Abstract

Poly(vinyl alcohol) (PVA) and carbon black (CB) nanoparticle-filled PVA nanofibers were successfully fabricated by electrospinning. The deposition area, morphological appearance, and diameters of the as-electrospun pristine PVA fibers were investigated to study the effects of solution concentration, preparation with sonication, applied electrostatic potential, and collection distance. The fibers that were fabricated according to the following conditions, i.e. 10% w/v PVA concentration, 15 kV applied voltage, and 15 cm collection distance, were chosen for the further study of the effects of CB composition on the morphological appearance and diameters of the as-electrospun CB-filled fibers. These nanofibers were also characterized by other techniques to investigate the effect of CB composition on chemical structure, crystallinity, and thermal properties of resulting fibers. Finally, the as-spun CB-loaded fibers were developed as an electroactive material through the investigation of mechanical and electrorheological properties. Interestingly, the obtained fibers had good tensile properties and could respond to an external electrical stimulation by displaying an increase in the modulus.

Key-words: electrospinning; nanofibers; carbon black; poly(vinyl alcohol)

4.2 Introduction

The exchange of electrical energy to mechanical energy or electromechanical energy conversion has been interested for many decades and has been applied in many applications such as muscle/insect-like actuators, catheter steering elements, miniature manipulators, dust-wipers, miniature robotic arms, and grippers [1-2]. Electroactive polymers (EAPs) are the important candidates of electromechanical energy conversion materials which offer promising and novel characters such as lightweight, high energy density, high response speed, and high flexibility [3]. The electro-viscoelastic elastomer is one type of electroactive polymers. Typically, it is a composite consisting of polarizable particles embedded in an insulating matrix, such as a gel or an elastomer. This material behaves like a fluid before crosslinking. An electric field is applied during curing to orient and to fix the position of the particles in the matrix. This material is changed into a solid state but still has shear moduli that may vary with applied electric field [4]. This system has several advantages as compared to other types of electroactive polymers such it has neither current leakage nor particle sedimentation, and it gives the right shape and size for the applications. However, the electric field application for orientation and the curing of the matrix for the position fixation of filled particles is seem to quite complicate. So, the development of an electroactive polymer that uses the same basic activation mechanism with electro-viscoelastic elastomer but use the easier method for fabrication is very interesting.

Recently, incorporation of a conductive polymer into a dielectric elastomer forming an electroactive composite has been of keen interest. Conductive polymers can offer a variety of benefits to the host elastomer: variable conductivity, better thermal stability, and mechanical properties [5]. Examples are polyanilene-polyisoprene composite for biosensor application [6] and polyanilene-EPDM composite for actuators application [7]. However, conductive polymers are the expensive materials. An alternative material that may be used instead conductive polymers is carbon black, an amorphous carbon in the form of near-spherical colloidal particles, because it has quite low cost, polasizable property, and very small size of particles.

Poly(vinyl alcohol) (PVA), a water-soluble polyhydroxy synthetic polymer, is a hydrophilic, semi-crystalline polymer that has received much interest in recent days

because of its good chemical and thermal stability, good physical properties, and complete biodegradability [8-9]. Moreover, PVA is one member of hydrogel or a three-dimensional network structure of a hydrophilic polymer capable of containing large amounts of water [10]. PVA can be called physical hydrogel because its three-dimensional network structures are not covalent bonds, but they come from the self formation of hydrogen bonds between polymer chains. From the above reasons, PVA may possible use as the matrix of electroactive polymer instead of an elastomer.

When the diameters of polymeric materials are shrunk to sub-micrometers or nanometers, there appear several amazing characteristics such as very large surface area to volume ratio, flexibility in surface functionalities, and superior mechanical performance compared with any other known form of the materials [11-12] because of the presence of tiny defects [13]. One of simple and versatile processing techniques that can be used to make ultrafine fiber which has received much attention in recent years is the electrostatic spinning or electrospinning; it is a process that utilizes high electrostatic potentials in fabricating ultrafine fibers [14]. Various materials have been successfully electrospun into ultrafine fibers, e.g. biopolymers, engineering plastics, conductive polymers, block copolymers, polymer blends, ceramics, and composite materials [15-17], mostly from polymer solutions or melts, including PVA. Over the past few years, many researchers have investigated various parameters affecting morphology and fiber diameter of electrospun PVA fibers, e.g. solution concentration, solution flow rate, degree of hydrolysis, applied electrical potential, collection distance, ionic salt addition [18], molecular weight of PVA [9,19-20], pH [21], surfactant addition [22], and type of collector [23], but none of them was reported in the effect on deposition area of electrospun fiber. Moreover, there are some researchers reported that electrospun PVA fibers can be used in several applications such as immobilization membranes of cellulose [24] and the protein delivery system [25], but none of them was reported in the applications of electroactive materials.

It is very interesting to use electrospinning to make the nanofibers from carbon black-loaded PVA composites and develop them to use as electroactive polymer by study their mechanical and electroactive properties. In the present contribution, therefore, we studied the electrospinning of the carbon black-filled electroactive electrospun polymeric nanofibers through mixing carbon black with PVA. An attempt was made to understand

the effects of solution properties (concentration and viscosity), experiment set ups (applied potential and collection distance), and carbon black composition on the morphological appearance, fiber diameter, and/or diameter of deposition area of the as-spun PVA fibers. The effects of carbon black composition on the mechanical and electrorheological properties of electrospun fibers were also investigated.

4.3 Experimental

4.3.1 Materials

Poly(vinyl alcohol) (PVA) powder [Mw = 72,000 Da; degree of hydrolysis (DH) \approx 97.5-99.5%, specific gravity = 1.25] was supplied from Fluka (Switzerland). The solvent used was reverse osmotic water which was filtered by Elix Millipore Z1XS5005Y reverse osmotic water filter. Carbon black (CB) nanoparticles (guaranteed particle size \approx 29 nm; specific gravity = 0.32) were supplied from East Asiatic Public (Thailand).

4.3.2 Preparation of Spinning Solutions

4.3.2.1 *Pristine PVA Spinning Solutions Preparation*

In order to establish a relationship between solution concentration and also applied potential; and morphological appearance and/or fiber diameter, pristine PVA was prepared in water with concentrations of 6, 8, 10, 12, and 14% (w/v). A weighed amount of PVA powder was dissolved in 40 ml warm water at 85°C in a 250-ml round bottom flask under slight stirring for 4 hr prior to electrospinning.

4.3.2.2 *Dispersion of CB and Preparation of CB-Load Spinning Solutions*

For CB loaded spinning solution preparation, the first important step is the dispersion of CB in water. The correct amount of CB was added to the 40 ml water in a 250-ml round bottom flask. The mixture was sealed tight and sonicated for 8 hr at 50°C. During this time, the suspension was vigorously shaken (manually) at every 2 hr interval and then stirred for 30 min at 85°C. This cycle was repeated 4 times. The required amount of PVA was then added to the mixture and allowed to dissolve with stirring at 85°C for 4 hr. After that each CB-loaded PVA solution was sonicated for 10 min at 50°C and was cooled down to room temperature.

In order to study the effect of CB composition, 10% (w/v) was chosen to be used as the concentration of PVA. Spinning solutions were prepared with CB contents of 0, 1, 2, 4, 6, 8, and 10 wt% (based on the weight of PVA powder). The summarized composition of the prepared spinning solutions are listed in Table 4.1. Prior to electrospinning, the as-prepared solutions were measured for their viscosity [at room temperature ($\sim 27^{\circ}\text{C}$)] and conductivity (at 25°C) using a Brookfield DV-III programmable viscometer and a Suntex SC 170 conductivity meter, respectively.

4.3.3 Electrospinning of Nanofibers

For electrospinning of pristine PVA solutions; in order to study the effects of solution concentration, applied potential, collection distance on the electrospinnability, morphological appearances, and/or fiber diameters; electrospinning was set-up with using the grounded target plate collector. Each of the as-prepared solutions was placed in a 50-ml plastic syringe. A 1.5-cm long, blunt-end stainless-steel gauge 20 needle (i.e. outside diameter = 0.91 mm) was used as the nozzle. The tilt angle of the syringe and the needle was 45° from a horizontal baseline to ascertain a constant presence of a solution droplet at the tip of the nozzle. A sheet of aluminum foil on a plastic backing was used as the grounded target plat collector. A Gamma High Voltage Research DES30PN/M692 power supply was used to generate a high DC potential across the needle (connected to the positive emitting electrode) and the collector (connected to the grounding electrode). The feed rate of the solutions for most experiments was controlled by means of a Kd Scientific syringe pump at 1 ml/hr. The as-spun products were kept in oven at 95°C for 24 hr prior to further characterization. For the study of effects of concentration and applied potential, spinning solutions at various concentrations in the range of 6 to 14% (w/v), which were prepared without sonication, were electrospun under various applied potentials in the range of 12.5 to 25 kV over a fixed collection distance of 15 cm. For the study of effects of collection distance, 10% (w/v) PVA solutions which were prepared with sonication were electrospun under a fixed applied potential of 15 kV over various collection distances in the range of 5 to 20 cm. For the study of effects of distance from the center of deposited area and CB composition, 10% (w/v) PVA solutions and CB-loaded PVA solutions at various CB contents, respectively, which were prepared with

sonication were electrospun under a fixed applied potential of 15 kV over a fixed collection distances of 15 cm. The collection time was fixed for all conditions at 1 min.

In order to fabricate the electrospun nanofiber mats for mechanical, electrorheological, and other characterization; the electrospinning was set-up similar to the previous mention except the collector, a rotating drum was used instead of the grounded target plat collector and the collection time was in the range of 24-48 hr (depend on the fixed thickness of electrospun mats at about 20-30 μm). The drum (outer diameter = 15 cm) rotated at an angular velocity of about 50 to 65 rpm.

4.3.4 Characterization of Pristine and CB-Loaded as-Spun PVA Nanofiber Mats, and/or CB

The morphological appearance of the as-spun fiber mats, CB, and as-cast CB-loaded PVA film were investigated by a JEOL JSM-5200 scanning electron microscope (SEM). The SEM images were obtained by using an acceleration voltage of 10 kV with a magnification of 200, 7,500 and/or 20,000x. The average fiber diameter of the electrospun fibers was measured by Semafore 4.0 software directly from SEM images at the magnification of 7,500x with at least 50 measurements.

A Perkin Elmer Pyris Diamond thermogravimetric-differential thermal analyser (TG-DTA) was used to determine amount of moisture content and decomposition temperature of CB, PVA powder, and as-spun fibers with the temperature scan from 30 to 1,000°C and a heating rate of 10°C/min.

A thermo Nicolet Nexus 670 Fourier-transformed infrared spectroscope (FT-IR) was used to identify the functional groups and chemical structure of the PVA powder, CB, as-spun PVA fibers, and as-spun CB-loaded PVA fibers. The measurements were operated with 32 scans and a resolution of $\pm 4\text{ cm}^{-1}$, covering a wavenumber range of 4000-400 cm^{-1} for direct transmission mode and 4000-650 cm^{-1} for horizontal attenuated total reflectance (HATR) mode.

The measurement of the crystallinity was carried out at room temperature with a Rigaku X-ray diffractometer, connected to a computer. For as-spun fiber mats, 4 layers of each sample were cut into a rectangular shape (2 cm x 2 cm) and laid on the rectangular (1.5 cm x 1.5 cm)-holed metal sample holder. For CB nanoparticles and PVA

powder, the samples were packed and smoothly swept off in the window of glass sample holder. The diffraction scans were collected at $2^\circ = 3-50^\circ$.

Mechanical integrity was investigated by using a Lloyd LRX universal testing machine. Mats of as-spun PVA and composite fibers were cut into a rectangular shape (6 mm x 70 mm) and placed on sample grippers. Testing was operated with gauge length of 50 mm and crosshead speed of 20 mm min⁻¹.

A Rheometric Scientific ARES melt rheometer with a thin fiber/film fixture was used to measure electrorheological properties of as-spun PVA and CB-loaded PVA fibers. A DC voltage was applied with an Instek GFG 8216A DC power supply. A digital multimeter was used to monitor voltage input. In these experiments, the dynamic tension strain was applied and the dynamic moduli [storage modulus (G') and lost modulus (G'')] were measured as functions of frequency and electric field strength. Mats of as-spun PVA and composite fibers (with thickness of 20-30 μm) were cut into a rectangular shape (6 mm x 70 mm) and placed on a film/fiber fixture sample holder which have the distance between two probes of 3 cm. Strain sweep tests were first carried out to determine the suitable strain to measure G' and G'' in the linear viscoelastic regime. The appropriate strain was determined to be 0.3% for all samples. Then frequency sweep tests were carried out to measure G' and G'' of each sample as functions of frequency. The deformation frequency was varied from 0.1 to 100 rad/s. Prior to each measurement, each samples were pre-tensioned at a low frequency (0.039811 rad/s), and then the electric field was applied for 10 minutes to ensure the formation of equilibrium polarization before each measurement was taken. Each measurement was carried out at room temperature ($\sim 27^\circ\text{C}$) and repeated at least two times.

4.4 Results and Discussion

4.4.1 Electrospinning of Electrospun Pristine PVA Fibers

To select the suitable electrospinning conditions producing the thinner and more uniform PVA nanofibers for using in fabrication of CB-loaded electrospun PVA fibers, a series of experiments with varying electrospinning parameters, including

solution concentration, applied potential, and collection distance were carried out. The results were shown and discussed in following sections.

For clearly understanding in explanation of electrospun results, first important point that should be mentioned is the story of forces acting on polymer jet in electrospinning. Typically, six types of forces are involved: they are electrostatic force which carries the charged jet from the nozzle to the screen collector, Coulombic repulsion force between adjacent charged species in a jet segment that is responsible for the stretching of the charged jet during its flight to the target, body or gravitational force, viscoelastic force which tries to prevent the charged jet from being stretched, surface tension, and drag force due to the friction between the charged jet and the surrounding air [26].

4.4.1.1 Effect of Solution Concentration

Solution concentration is one of the most important parameters in electrospinning, due to its effect on viscosity, as shown in Table 4.2 (a-e), the viscosity increased monotonously with increasing solution concentration. It was well known that to prepare fibers by electrospinning, a proper solution concentration and hence the resulting viscosity is required. If the solution concentration is too low, a continuous stream of charged liquid (i.e. charged jet) cannot be formed as the charged jet ultimately undergoes an instability flow that results in the formation of droplets, a process traditionally known as electrospraying [27]. In the other word, a critical polymer solution concentration needed to be exceeded as extensive chain entanglements are necessary to produce electrospun fibers. Below this concentration, chain entanglements were insufficient to stabilize the jet and the contraction driven by the surface tension caused the solution to form beads or beaded fibers. However, if the solution concentration becomes too great, electrospinning is also prohibitive as a continuous flow of the polymer liquid from the tip of the nozzle is somewhat restricted. As a result, there is a limited concentration or viscosity range within which a polymer solution can be electrospinnable. Beyond this range (either higher or lower), discrete droplets are likely to occur [28].

A series of pristine PVA solutions at various PVA concentrations in the range of 6-14% (w/v) which prepared without sonication were electrospun, resulting in fiber morphology and diameter as shown in the selected SEM images in Figure 4.1 and illustrated in Figure 4.2, respectively. Irrespective of the applied potential, at the lowest

concentration [6% (w/v)], T-shape and spindle-like beads fibers were obtained due to low entanglement of polymer chains and the average fiber diameters between beads were very small in the range of 85-105 nm. With increasing concentration, the morphology of fibers was changed from beaded fiber to uniform fiber and fiber diameter was also gradually increased to the range of 486-647 nm at the highest concentration [14% (w/v)].

Table 4.3 shows the selected optical images illustrate the deposition area of the as-spun fibers from 6-14% (w/v) PVA solutions and quantitative results are summarized in Table 4.4. The results show that, not only morphological appearance and diameter, but solution concentration can also affect to the deposition area of electrospun fibers. With increasing concentration, the deposition area was found to decrease. The increase of viscosity and conductivity of solution with increasing concentration (see Table 4.2) should be responsible for this observation, because greater conductivity leads to greater electrostatic force (responsible for rapid carrying the charged jet to the collective target) while greater viscosity leads to greater viscoelastic force (responsible for preventing the charged jet from being stretched) [26]. This positively confirms the postulation given above.

4.4.1.2 Effect of Applied Voltage

In order to investigate the effect of applied potential on morphological appearance, size, and deposition area of the as-spun fibers, the as-prepared PVA solutions were electrospun at various applied electrostatic potentials in the range of 12.5-25 kV and collection distance was held at 15 cm. Selected SEM images of as-spun fibers obtained and quantitative analysis are shown in Figures 1 and 2, respectively. For the beaded fibers, the shape of beads was found to change from T-shape to spindle-like and the size of beads was found to decrease with increasing applied voltage. Evidently, the number of fibers per unit area was found to increase with increase in the applied voltage. Moreover, not like any literature [18,20], the size of the as-spun fibers and its variation was generally found to decrease with initial increase in the applied potential, reach a minimum at an immediate value, and increase with further increase in the applied potential. This trend can be more obviously observed if the solution concentration was increased.

At a given concentration, the increase in the applied potential could result in an increase in total number of charged species within a jet segment, hence an

increase in both the electrostatic and the Coulombic repulsion forces. The increase in the Coulombic repulsion force should be responsible for the observed decrease in the size of the beaded fibers and as-spun fibers, while the increase in the electrostatic force could contribute to the observed increase in the size of the as-spun fibers. The increase in the size of the as-spun products due to the increased electrostatic force should be caused by two different phenomena. The first is due to the decrease in the total path trajectory that the jet travels from the nozzle to the screen collector, a result of the increase in the speed of the jet, while the second is due to the increase in the total feed flow rate. Consequently, whether the as-spun products should be increase or decrease in their size depends totally on the competition between these two effects. This postulation can also describe the formation of some small fibers and the observation of wide size variation at high applied potential. For deposition area (see Table 4.3 and 4.4), it was found that the deposition area gradually decrease with increase in applied potential, illustrate that the electrostatic force has more effect on deposition area than the Coulombic repulsion force.

4.4.1.3 Effect of Sonication in Preparation of Solution

Sonication is required for dispersion of CB in PVA solution, so the study of the effect of sonication on fiber diameter is necessary. In order to do that, electrospinning of 10% (w/v) pristine PVA solution with and without sonication for 10 min were carried out under applied voltage of 15kV over a fixed collection distance of 15 cm. After sonication, viscosity of solution was found to decrease from 810 to 604 mPa.s while conductivity was not found to change (remain at 1.011 mS/cm) [see Table 4.2 (c-f)]. The reducing in molecular weight of PVA under sonication should be responsible for the observed lower viscosity of polymer solution. Although not shown here, it was observed that the diameter of as-spun fibers from sonicated solution was smaller than from pristine solution (169 ± 15 and 285 ± 34 nm), as a result of lower viscosity and same conductivity. Lower viscosity leads to lower viscoelastic force so the charged jet was stretched easily, while remained high conductivity leads to great electrostatic force pull the charged jet to the collector.

4.4.1.4 Effect of Collection Distance

In order to study the effect of collection distance, the as-prepared 10% (w/v) PVA solutions which were prepared with sonication were electrospun under applied voltage of 15kV over various collection distances in the range of 5-20. Selected

SEM images of the as-spun fibers obtained and quantitative analysis plot are shown in Figures 3 and 4, respectively. At a collection distance of 5 cm, the electrospun results showed wet pattern and bead formation, which attributed to the incompletely solidification and instability stretching during the electrospinning. As the collection distance was increased, the average diameters of the nanofiber were decreased because of the increasing in distance for instability stretching until the collection distance of 15 cm, the images were undistinguishable for electrospinning over further increasing in collection distance. It could be assumed that solution jets were elongated and solidified completely before deposited. For deposition area, it was observed that the deposition area gradually increase with increase in collection distance (see Table 4.5), on the other hand, the number of fiber per unit area was found to decrease with increase in the collection distance (see Figure 4.3), most likely a result of increasing in distance for instability stretching.

4.4.1.5 Distance from the Center of Deposition Area

Figure 4.5 shows selected SEM images of as-spun fibers from sonicated 10% (w/v) PVA solutions which were collected from various distances far from the center of deposition area. The as-spun fibers were found to looser with increasing in distance from the center of deposition area. For fiber diameter, fiber diameters were not found to change (about 169 nm) while size variation was found to decrease with increasing in distance from the center of deposition area (see Figure 4.6). The wide size variation could be described when observe as-spun fibers at low magnification. Outside the deposition area (radius of deposition area was 7.5 cm) [see Figure 4.5 (d) and (e)], some as-spun fibers were observed in the forms of some line deposition patterns and many small loops which attributed to two series of bending instability of the highly charged jet, primary and secondary bending instability, respectively. Actually, line deposition patterns are one part of big loop-deposited fibers came from the moving of charged jet driven by primary bending instability. Secondary bending instability caused a small loop-like moving before deposition and further size reduction. Wide size variation in deposition area of as-spun fibers was a result of combination of deposited fibers from primary and secondary bending instability.

4.4.2 Electrospinning of CB-Loaded Electrospun PVA Fibers (Effect of CB Composition)

The CB-loaded 10% (w/v) PVA solutions at various contents of CB were prepared by dispersion CB in PVA solutions by stirring and sonication. The incorporation of CB slightly increase the viscosity and conductivity of PVA solution as see in Table 4.2 (f-1). In order to investigate the effect of CB composition on morphological appearance and size of the as-spun fibers, the as-prepared CB-loaded 10% (w/v) PVA solutions at various contents of CB were electrospun. The SEM observation results were shown in Figure 4.7. Not uniform surface was found to increase with increasing in CB contents due to harder dispersion of CB in increasing of CB content. Generally, it was reported in many literatures that even with the high intensity ultrasonic agitation, complete aggregates disassociation apparently was not realized [29-30]. Table 4.6 shows the deposition area results from this study. It was observed that the deposition area a little bit decrease with increase in CB content due to slightly in crease in viscosity and conductivity.

4.4.3 Characterization of CB-Loaded Electrospun PVA Fibers

Shown in Table 4.7 are optical images of as-spun fiber mats at various CB contents ranging from 0-10 wt% (with respect to PVA). The uniformly grey scale provides an early indication of the incorporation of CB in the electrospun nanofiber mats.

TGA was use to study thermal properties and confirm the presence of CB in the electrospun fibers. Figure 4.8 (a) illustrates TGA thermograms for PVA powder and as-spun pristine PVA mats. For both samples, four steps of weight loss were observed. The first covered the temperature range of abou: 30 to 90°C, corresponding to the loss of moisture, while the second, third, and forth covered the temperature ranges of about 220 to 340, 340 to 470, and 720 to 890°C, corresponding to the thermal degradation of PVA. Figure 4.8 (b) illustrates TGA thermograms for CB and as-spun CB-loaded PVA mats at various CB contents. CB exhibited two steps of weight loss covering the temperature ranges of about 30 to 90°C and the onset of about 620°C, corresponding to the loss of moisture and the thermal degradation of some functionality in CB, respectively. For as-spun CB-loaded PVA mats at CB contents of 1-6 wt%, the reduction of weight loss at the

temperature range of about 220 to 340°C and 340 to 470°C; the disappearance of weight loss at the temperature range of about 720 to 890°C, and the new weight loss step at temperature range of about 470 to 570 °C were observed. For increase in CB contents to 8 and 10 wt%, last step of degradation was increased from about 470 to 570 °C to the onset of about 750°C. It can conclude that, CB can improve the thermal stability of as-spun PVA fiber at the latter step of degradation. In addition, the percentage residual as compared to percentage weight loss of PVA is corresponding to the composition of CB in as-spun CB-loaded PVA mats.

FT-IR in HATR mode was used to identify the chemical structure and observe any change in the crystallinity of as-spun CB-loaded PVA fibers. The results were shown in Figure 4.9. IR spectrum of as-spun pristine PVA fibers exhibited the characteristic peak at 3300 cm^{-1} , corresponding to the stretching vibration band of hydrogen-bonded alcohol (-OH) [31]. IR spectra of as-spun fibers was not found to change with increasing in percentage contents of CB, illustrates that no change in structure of PVA with increasing in CB contents. Moreover, it is well known that the adsorption peak at 1144 cm^{-1} [C-O of doubly H-bonded OH in crystalline regions [32]] is useful for indication of the crystallinity of PVA. Apparently, the relative intensity of this peak was not found to change with increasing CB content, indicates that incorporation of CB did not have any effect on the crystallinity of the PVA matrix.

The crystallinity of electrospun fibers may be of primary importance when applications were considered. Figure 4.10 shows WAXD patterns of PVA powder, as-spun PVA fibers, as-spun CB-loaded PVA composite fibers, and CB nanoparticles. The reflections of the CB pattern [Figure 4.10 (i)] were broad due to CB is the amorphous carbon. Compared with those of the PVA powder [Figure 4.10 (a)], the peak appeared at the same position ($2\theta \approx 20^\circ$) while the reflections of the as-spun PVA fiber pattern [Figure 4.10 (b)] were relatively broad and strong. Meanwhile, the WAXD pattern of the PVA powder also contained numerous higher order reflections that could not be seen in the fiber pattern [20,33]. The broad and strong nature of the PVA fiber pattern reflections indicated that the crystalline microstructure in the electrospun fibers was significantly greater than that in the PVA powder. Apparently, the relative intensity and position of the peak of pattern was not found to change with increase in CB content [Figure 4.10 (c-h)],

indicates that incorporation of CB did not have any effect on the crystallinity of the PVA matrix. This result is corresponding to FT-IR result.

4.4.4 Mechanical Properties

Table 4.8 summarize some mechanical properties of as-spun CB-loaded PVA fiber mats having different CB contents. The results suggested that with the addition of CB, the modulus of as-spun fiber mat were found to generally increase reach to a value, and at the highest CB contents, the elastic modulus found to decrease due to hard dissociation of carbon black aggregates. Close inspection of our data suggests that CB nanoparticles in the polymer acted as fillers in the matrix like the behavior in general CB composites or CB-filled rubber, CB-PVA interaction mechanism may be based on the physical entrapment of the PVA chains in the carbon black microstructural defects and superficial porosities [34]. However, the maximum stress and strain at break were found to decrease with increase in CB contents. It could be attributed to non uniform dispersion and increasing number of CB aggregates in the spinning solution during electrospinning.

4.4.5 Electrorheological Properties

The effect of electric field strength on the rheological properties of as-spun CB-loaded PVA fibers, at various CB contents, was investigated under electric field strength between 0-130 V/mm. Not shown here, the storage modulus [$E'(\omega)$] and loss modulus [$E''(\omega)$] of each specimen generally increased with increase in the electric field strength. Figure 4.11 shows the storage and loss modulus responses [$\Delta E'$ and $\Delta E''$, respectively) of as-spun CB-loaded PVA electrospun nanofiber mats at various CB contents as functions of electric field strengths at frequency 1.0 rad/s and strain 0.3%. The storage and loss modulus responses appear to increase linearly with electric field reach a maximum at an immediate value, and constant with further increase in the electric field strength. For the effect of CB contents, at the steady state (at electric field strength of 100 V/mm), the storage and loss modulus responses was found to increase with increase in CB content as shown in Figure 4.12. The corresponding storage sensitivity, defined as $\Delta E'(\omega) / \Delta E'_0(\omega)$, of the as-spun CB-loaded PVA fibers at various CB contents at electric field strength of 100 V/mm were found to high and increase with increase in

CB contents [$\Delta E'(\omega)/E'_0(\omega) = 41, 48, \text{ and } 84\%$ for 0, 1, and 10 wt% CB, respectively]. These phenomena can describe by following reasons. For the response of as-spun pristine PVA fibers, as an electric field is applied, electrical dipole moments are generated and the electrostatic interaction between PVA chains are induced leading to intermolecular interaction acting like an electrical network combined to former H-bonding network. The intermolecular interaction and the electrostatic interaction result in the loss of chain free movements, the higher chain rigidity, and as a result the higher $E'(\omega)$. Moreover, a voltage differential between the electrodes is known creates electromagnetic forces that act to pull the electrodes together [35] can also affect to response of materials under electric field. For the better response of as-spun CB-loaded PVA fibers, as the electrical field was applied both CB nanoparticles and PVA became polarized and induced dipole moments were generated, leading to more intermolecular interactions, as indicated by a higher modulus, this result consistent with the results of conductive polymer/elastomer system [35-36].

4.5 Conclusions

In this study, poly(vinyl alcohol) (PVA) and carbon black (CB) nanoparticle-filled PVA nanofibers were successfully fabricated by electrospinning with the fiber sizes of about 85-647 and 169 nm, respectively. The deposition area, morphological appearance, and diameters of the as-electrospun pristine PVA fibers were investigated to study the effects of solution concentration, preparation with sonication, applied electrostatic potential, and collection distance. The results show that, bead formation and deposition area were found to decrease while fiber diameter was found to increase with increasing solution concentration. Deposition area was found to decrease with increasing applied potential while fiber diameter was found to decrease to a minimum value and then increase. Fiber diameter was found to decrease with the preparation of spinning solution with sonication. Deposition area was found to increase with increasing collection distance while fiber diameter was found to decrease to a value and then constant. Fiber diameter was not found to change with increase in distance from the center of deposition area while its variation was found to decrease. The fibers that were fabricated according to the following conditions, i.e. 10% w/v PVA concentration, 15 kV applied voltage, and

15 cm collection distance, were chosen for the further study of the effects of CB composition on the morphological appearance and diameters of the as-electrospun CB-filled fibers. Fiber diameter was not found to change with increasing of CB contents while deposition area was found to slightly decrease. These nanofibers were also characterized by other techniques to investigate the effect of CB composition on chemical structure, crystallinity, and thermal properties of resulting fibers. CB was not found to change in structure and crystallinity to PVA matrix, but it can increase in grey color and thermal stability of PVA matrix. Finally, the as-spun CB-loaded fibers were developed as an electroactive material through the investigation of mechanical and electrorheological properties. Interestingly, the obtained fibers had good tensile properties and could respond to an external electrical stimulation by displaying an increase in the modulus.

4.6 Acknowledgments

The authors acknowledge partial support received from 1) the National Research Council of Thailand (NRCT), 2) Chulalongkorn University (through a grant from the Ratchadapesek Somphot Endowment Fund provided to the Conductive and Electroactive Polymers Research Unit), 3) the Petroleum and Petrochemical Technology Consortium [through a Thai governmental loan from Asian Development Bank (ADB)], and 4) the Petroleum and Petrochemical College (PPC), Chulalongkorn University. Lastly, the authors would like to thank Dr. Ladawan Wannatong for carrying of carbon black sample.

4.7 References

- [1] Krause S and Bohon K 2001 Electromechanical response of electrorheological fluids and poly(dimethylsiloxane) networks *Macromolecules* **34** 7179-7189
- [2] Shahinpoor M 2003 Ionic polymer-conductor composites as biomimetic sensors, robotic actuators and artificial muscles-a review *Electrochimica Acta* **48** 2343-2353
- [3] Bar-Cohen Y, Xue T, Shahinpoor M, Harrison J S and Smith J G 1998 Low-mass muscle actuators using electroactive polymers (EAP) *Smart Structures and Materials 1998: Smart Materials Technologies, Proc. SPIE* **3324** 218-223
- [4] Mak C S and Kosmatka J B 2002 A new method for characterizing the dynamic properties of electroviscoelastic materials *Smart Structures and Materials 2002: Electroactive Polymer Actuators and Devices, Proc. SPIE* **4695** 277-285
- [5] Sankır M, Küçükyavuz S and Küçükyavuz Z 2002 Electrochemical preparation and characterization of carbon fiber reinforced poly(dimethylsiloxane)/polythiophene composites: electrical, thermal and mechanical properties *Synthetic Metals* **128** 247-251
- [6] Xue H, Shen Z and Li Y 2001 Polyaniline-polyisoprene composite film based glucose biosensor with high permselectivity *Synthetic Metals* **124** 345-349
- [7] Faez R, Schuster R H and De Paoli M-A 2002 A conductive elastomer based on EPDM and polyaniline: II. Effect of the crosslinking method *European Polymer Journal* **38** 2459-2463
- [8] DeMerlis C C and Schoneker D R 2003 Review of the oral toxicity of polyvinyl alcohol (PVA) *Food and Chemical Toxicology* **41** 319-326
- [9] Koski A, Yim K and Shivkumar S 2004 Effect of molecular weight on fibrous PVA produced by electrospinning *Materials Letter*. **58** 493-497
- [10] Kim S J, Park S J, An K H, Kim N G and Kim S I 2003 Water behavior of poly(vinyl alcohol)/poly(vinylpyrrolidone) interpenetrating polymer network hydrogels *Journal of Apply Polymer Science* **89** 24-27
- [11] Lu J Y, Normal C, Abboud K A and Ison A 2001 Crystal engineering of an inclusion coordination polymer with cationic pocket-like structure and its property to form metal-organic nanofibers *Inorganic Chemistry Communications* **4** 459-461

- [12] Doshi J and Reneker D H 1995 Electrospinning process and applications of electrospun fibers *Journal of Electrostatics* **35** 151-160
- [13] Griffith A A 1921 The Phenomena of Rupture and Flow in Solids *Philosophical Transactions of the Royal Society of London. Series A* **221** 163-198
- [14] Huang Z M, Zhang, Y -Z, Kotaki M and Ramakrishna S 2003 A review on polymer nanofibers by electrospinning and their applications in nanocomposites *Composites Science and Technology* **63** 2223-2253
- [15] Jayaraman K, Kotaki M, Zhang Y, Mo X and Ramakrishna S 2004 Recent advances in polymer nanofibers *Journal of Nanoscience and Nanotechnology* **4** 52-65
- [16] Reneker D H and Chun I 1996 Nanometre diameter fibres of polymer, produced by electrospinning *Nanotechnology* **7** 216-223
- [17] Li D and Xia Y 2004 Electrospinning of nanofibers: reinventing the wheel *Advanced Materials* **16** 1151-1170
- [18] Zhang C, Yuan X, Wu L, Han Y and Sheng J 2005 Study on morphology of electrospun poly(vinyl alcohol) mats *European Polymer Journal* **41** 423-432
- [19] Jun Z, Hou H, Wendorff H J and Greiner A 2005 Poly(vinyl alcohol) nanofibres by electrospinning: influence of molecular weight on fibre shape *e-Polymer* **38** 1-7
- [20] Lee J S, Choi K H, Ghim H D, Kim S S, Chun D H, Kim H Y and Lyoo W S 2004 Role of molecular weight of atactic poly(vinyl alcohol) (PVA) in the structure and properties of PVA nanofabric prepared by electrospinning *Journal of Applied Polymer Science* **93** 1638-1646
- [21] Son W K, Youk J H, Lee T S and Park W H 2005 Effect of pH on electrospinning of poly(vinyl alcohol) *Materials Letters* **59** 1571-1575
- [22] Yao L, Haas T W, Guiseppi-Elie A, Simpson D G, Bowlin G L and Wnek G E 2003 Electrospinning and stabilization of fully hydrolyzed poly(vinyl alcohol) fibers *Chemistry of Materials* **15** 1860-1864
- [23] Chuangchote S and Supaphol P 2006 Fabrication of aligned poly(vinyl alcohol) nanofibers by electrospinning *Journal of Nanoscience and Nanotechnology* **6** 125-129
- [24] Wu L, Yuan X and Sheng J 2005 Immobilization of cellulase in nanofibrous PVA membranes by electrospinning *Journal of Membrane Science* **250** 167-173

- [25] Zeng J, Aliger A, Czubyko F, Kissel T, Wendorff J H and Greiner A 2004 Poly(vinyl alcohol) nanofibers by electrospinning as a protein delivery system and the retardation of enzyme release by additional polymer coatings *Biomacromolecules* **6** 1484-1488
- [26] Wannatong L, Sirivat A and Supaphol P 2004 Effects of solvents on electrospun polymeric fibers: preliminary study on polystyrene *Polymer International* **53** 1852-1859
- [27] Pantano C, Gañán-Calvo A M and Barrero A 1994 Zeroth-order, electrohydrostatic solution for electrospraying in cone-jet mode *Journal of Aerosol Science* **25** 1065-1077
- [28] Lee K H, Kim H Y, Bang H J, Jung Y H and Lee S G 2003 The change of bead morphology formed on electrospun polystyrene fibers *Polymer* **44** 4029-4034
- [29] Pomchaitaward C, Manas-Zloczower I and Feke D L 2003 Investigation of the dispersion of carbon black agglomerates of various sizes in simple-shear flows *Chemical Engineering Science* **58** 1859-1865
- [30] Jäger K -M and McQueen D H 2001 Fractal agglomerates and electrical conductivity in carbon black polymer composites *Polymer* **42** 9575-9581
- [31] Kuptsov A H and Zhizhin G N 1998 *Handbook of Fourier Transform Raman and Infrared Spectra of Polymers* Amsterdam: Elsevier
- [32] Sriupayo J, Supaphol P, Blackwell J and Rujiravanit J 2005 Preparation and characterization of alpha-chitin whisker-reinforced poly(vinyl alcohol) nanocomposite films with or without heat treatment *Polymer* **46** 5637-5644
- [33] Ding B, Kim H Y, Lee S C, Shao C L, Lee D R, Park S J, Kwag G B and Choi K J 2002 Preparation and characterization of a nanoscale poly(vinyl alcohol) fiber aggregate produced by an electrospinning method *Journal of Polymer Science: Part B: Polymer Physics* **40** 1261-1268
- [34] Baccaro S, Cataldo F, Cecilia A, Cemmi A, Padella F and Santini A 2003 Interaction between reinforce carbon black and polymeric matrix for industrial applications *Nuclear Instruments and Methods in Physics Research Section B: Beam Interactions with Materials and Atoms* **208** 191-194

- [35] Pelrine R E, Kornbluh R D and Joseph J P 1998 Electrostriction of polymer dielectrics with compliant electrodes as a means of actuation *Sensors and Actuators A: Physical* **64** 77-85
- [36] Liu B and Shaw M T 2001 Electrorheology of filled silicone elastomers *Journal of Rheology* **45** 641-657

Table 4.1 Composition of CB in various CB-loaded spinning solutions

Sample	wt% (based on the weight of PVA powder)		% (w/w) (based on the weight of solid content)		% (v/v) (based on the volume of solid content)	
	CB	PVA	CB	PVA	CB	PVA
0 CB-PVA	0	100	0.0	100.0	0.0	100.0
1 CB-PVA	1	100	1.0	99.0	3.8	96.2
2 CB-PVA	2	100	2.0	98.0	7.2	92.8
4 CB-PVA	4	100	3.8	96.2	13.5	86.5
6 CB-PVA	6	100	5.7	94.3	19.0	81.0
8 CB-PVA	8	100	7.4	92.6	23.8	76.2
10 CB-PVA	10	100	9.1	90.9	28.1	71.9

Table 4.2 Some properties of pristine PVA and CB-loaded solutions

	PVA concentration [% (w/v)]	CB contents [wt% (base on weigh of PVA)]	Sonication	Viscosity (mPa.s)	Conductivity (mS/cm)
(a)	6	-	No	62	0.727
(b)	8	-	No	181	0.865
(c)	10	-	No	810	1.011
(d)	12	-	No	1932	1.215
(e)	14	-	No	2430	1.267
(f)	10	0	Yes	604	1.011
(g)	10	1	Yes	601	1.013
(h)	10	2	Yes	605	1.015
(i)	10	4	Yes	610	1.017
(j)	10	6	Yes	614	1.020
(k)	10	8	Yes	618	1.021
(l)	10	10	Yes	620	1.024

Table 4.3 Selected optical images illustrate the deposition area of the as-spun fibers from 6-14% (w/v) PVA solutions. The applied potentials were varied between 12.5 and 25.0 kV over a fixed collection distance of 15 cm and the feed flow rate was 1 ml/hr

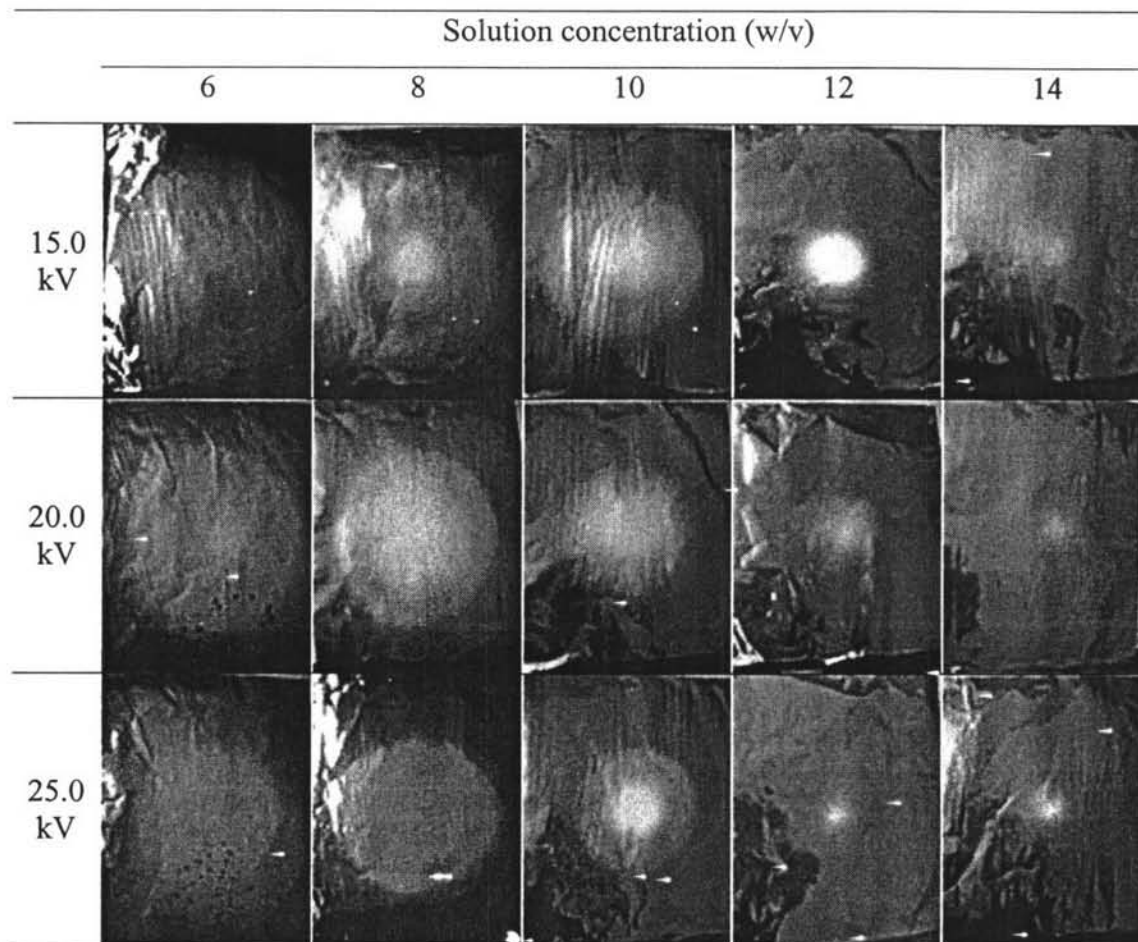


Table 4.4 Average deposition diameter (cm) of the as-spun fibers from 6-14% (w/v) PVA solutions. The applied potentials were varied between 12.5 and 25.0 kV over a fixed collection distance of 15 cm and the feed flow rate was 1 ml/hr

Applied voltage (kV)	Solution concentration (w/v)				
	6	8	10	12	14
12.5	22.0	19.5	18.0	12.0	10.0
15.0	20.0	19.0	15.0	7.5	6.5
17.5	19.0	17.5	13.5	7.0	5.0
20.0	17.0	15.0	12.5	6.0	3.2
22.5	15.5	13.5	12.0	4.5	4.5
25.0	13.0	12.5	11.5	4.0	4.5

Table 4.5 Selected optical images and analyzed diameters (D) of deposition area of the as-spun fibers from as-prepared-sonicated 10% (w/v) PVA solutions. The applied potential was 15 kV over various collection distances in the range of 5-20 cm and the feed flow rate was 1 ml/hr




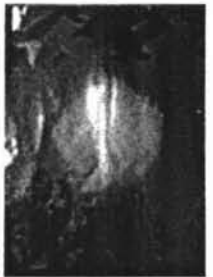



Collection distance (cm)			
5.0	7.5	10.0	12.5
			
D = 3 cm	D = 4.5 cm	D = 6.5 cm	D = 9 cm
Collection distance (cm)			
15.0	17.5	20.0	
			
D = 12 cm	D = 13.5 cm	D = 17 cm	

Table 4.6 Selected optical images and analyzed diameters (D) of deposition area of the as-spun fibers from as-prepared CB-loaded 10% (w/v) PVA solutions at various CB contents. The applied potential was 15 kV over various collection distances in the range of 5-20 cm and the feed flow rate was 1 ml/hr. Collection time was 5 min

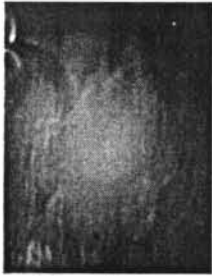






CB contents (wt%) (base on the weight of PVA)			
0	1	2	4
			
D = 16 cm	D = 15 cm	D = 14.5 cm	D = 14 cm
CB contents (wt%) (base on the weight of PVA)			
6	8	10	
			
D = 14 cm	D = 13.5 cm	D = 12 cm	

Table 4.7 Optical images of the as-spun fiber mats from as-prepared CB-loaded 10% (w/v) PVA solutions at various CB contents. The applied potential was 15 kV over collection distance of 15 cm. The feed flow rate was 1 ml/hr. Original magnification = 20kx and scale bar = 1 μ m. Collection time was 24-48 hr








CB contents (wt%) (base on the weight of PVA)						
0	1	2	4	6	8	10
						

Table 4.8 Mechanical properties of as-spun CB-loaded fiber mats having different CB contents

CB contents (wt%) (base on the weight of PVA)	Elastic modulus (Mpa)	Maximum stress (Mpa)	Strain at break (%)
0	80.6 ± 27.2	7.37 ± 2.7	162.2 ± 37.4
1	85.4 ± 13.1	6.29 ± 3.9	115.7 ± 32.8
2	96.3 ± 10.4	6.98 ± 3.4	84.3 ± 11.1
4	127.8 ± 27.5	5.54 ± 2.1	58.8 ± 15.3
6	157.1 ± 10.1	4.56 ± 2.2	58.7 ± 13.7
8	162.5 ± 27.6	4.49 ± 3.5	27.1 ± 5.9
10	155.6 ± 29.8	4.44 ± 1.4	22.9 ± 9.8

4.8 Caption of Figures

- Figure 4.1** Selected SEM images of the as-spun fibers from (a) 6, (b) 8, (c) 10, (d) 12, and (e) 14% (w/v) PVA solutions. “1”, “2”, and “3” represent the applied potentials of 12.5, 17.5, and 22.5 kV, respectively, over a collection distance of 15 cm. The feed flow rate of solution was 1 ml/hr. Original magnification = 7,500x and scale bar = 1 μm .
- Figure 4.2** Average diameters (μm) of the as-spun fibers from PVA solutions at concentration of (●) 6, (■) 8, (▲) 10, (▼) 12, and (◆) 14% (w/v). The applied potentials were varied between 12.5 and 25.0 kV over a fixed collection distance of 15 cm and the feed flow rate was 1 ml/hr.
- Figure 4.3** Selected SEM images of the as-spun fibers from sonicated 10% (w/v) PVA solutions. The applied potential was 15 kV over varied collection distance of (a) 5, (b) 10, (c) 15, and (d) 20 cm. The feed flow rate was 1 ml/hr. Original magnification = 7,500x and scale bar = 1 μm .
- Figure 4.4** Average diameters (μm) of the as-spun fibers from sonicated 10% (w/v) PVA solutions. The applied potential was 15 kV over varied collection distance in the range of 5-20 cm and the feed flow rate was 1 ml/hr.
- Figure 4.5** Selected SEM images of the as-spun fibers from sonicated 10% (w/v) PVA solutions which were collected from distances of (1) 0, (2) 3, (c) 6, (d) 9, and (e) 12 cm far from the center of deposition area. The applied potential was 15 kV over collection distance of 15 cm. The feed flow rate was 1 ml/hr. Original magnification = 200x and scale bar = 100 μm .
- Figure 4.6** Average diameters (μm) of the as-spun fibers from sonicated 10% (w/v) PVA solutions which were collected from various distances far from the center of deposition area. The applied potential was 15 kV over collection distance of 15 cm. The feed flow rate was 1 ml/hr.
- Figure 4.7** Selected SEM images of the as-spun fibers from as-prepared CB-loaded 10% (w/v) PVA solutions at CB contents of (a) 0, (b) 1, (c) 2, (d) 4, (e) 6, (f) 8, and (g) 10 wt% (base on the weight of PVA). The applied potential

was 15 kV over collection distance of 15 cm. The feed flow rate was 1 ml/hr. Original magnification = 20kx and scale bar = 1 μm .

- Figure 4.8** TGA thermograms of (a) PVA powder and as-spun pristine PVA fibers; and (b) CB and as-spun CB-loaded PVA fiber at various content of CB.
- Figure 4.9** IR spectra of as-spun CB-loaded PVA fibers at various CB contents.
- Figure 4.10** WAXD patterns of: (a) PVA powder; (b) as-spun PVA fibers; (c-h) 1, 2, 4, 6, 8, 10 wt% as-spun CB-loaded (base on weight of PVA) PVA fibers, respectively; and (i) CB nanoparticles.
- Figure 4.11** Responses of the modulus of as-spun CB-loaded PVA fibers at various electric field strength and various compositions of CB, frequency = 1.0 rad/s and strain = 0.3 % at 27°C: (a) storage modulus [$\Delta E'(w)$] and (b) loss modulus [$\Delta E''(w)$].
- Figure 4.12** Responses of the modulus of as-spun CB-loaded PVA fibers at electric field = 100 V/mm: (a) storage modulus [$\Delta E'(w)$] and (b) loss modulus [$\Delta E''(w)$].

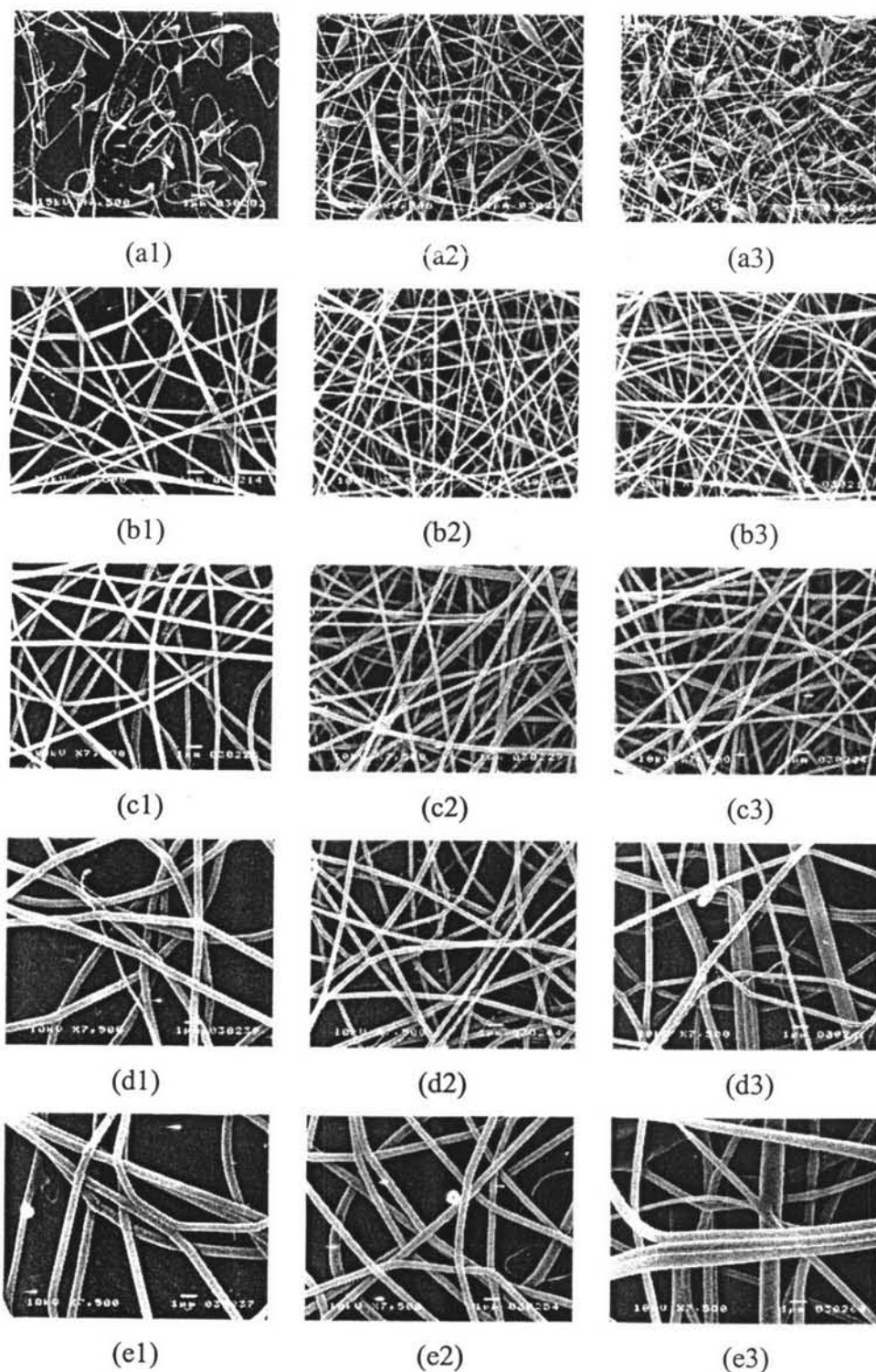


Figure 4.1 Selected SEM images of the as-spun fibers from (a) 6, (b) 8, (c) 10, (d) 12, and (e) 14% (w/v) PVA solutions. “1”, “2”, and “3” represent the applied potentials of 12.5, 17.5, and 22.5 kV, respectively, over a collection distance of 15 cm. The feed flow rate of solution was 1 ml/hr. Original magnification = 7,500x and scale bar = 1 μ m.

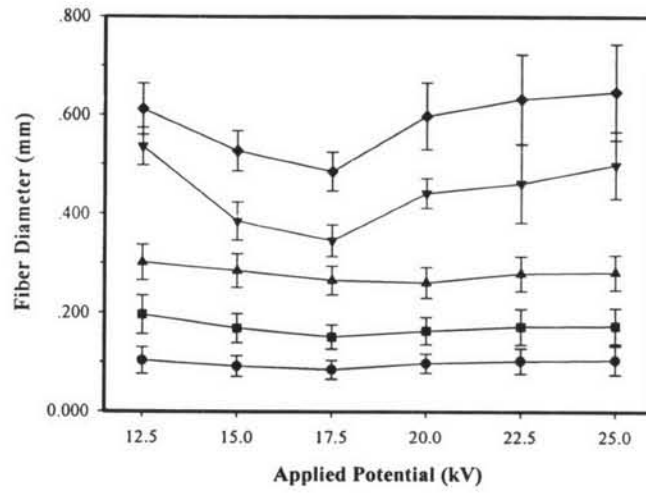


Figure 4.2 Average diameters (μm) of the as-spun fibers from PVA solutions at concentration of (●) 6, (■) 8, (▲) 10, (▼) 12, and (◆) 14% (w/v). The applied potentials were varied between 12.5 and 25.0 kV over a fixed collection distance of 15 cm and the feed flow rate was 1 ml/hr.

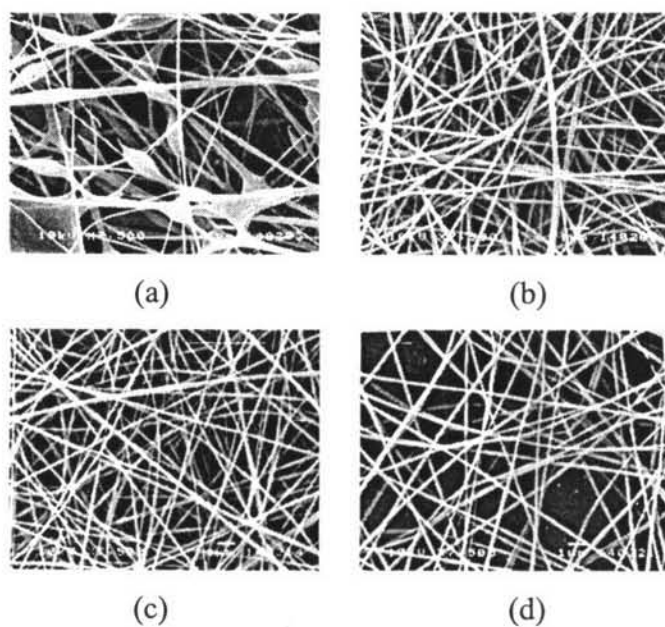


Figure 4.3 Selected SEM images of the as-spun fibers from sonicated 10% (w/v) PVA solutions. The applied potential was 15 kV over varied collection distance of (a) 5, (b) 10, (c) 15, and (d) 20 cm. The feed flow rate was 1 ml/hr. Original magnification = 7,500x and scale bar = 1 μm .

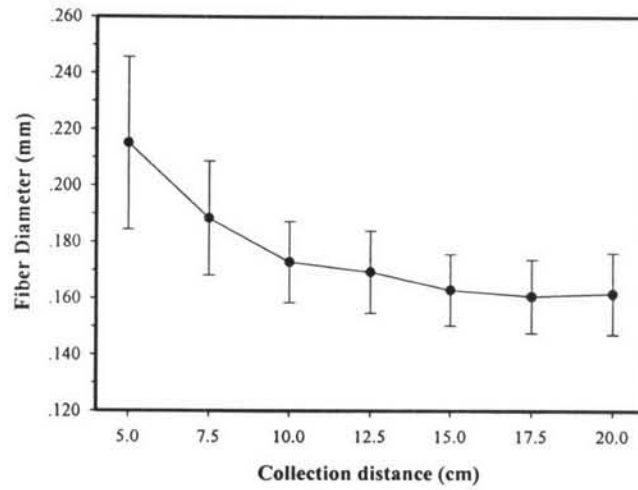


Figure 4.4 Average diameters (μm) of the as-spun fibers from sonicated 10% (w/v) PVA solutions. The applied potential was 15 kV over varied collection distance in the range of 5-20 cm and the feed flow rate was 1 ml/hr.

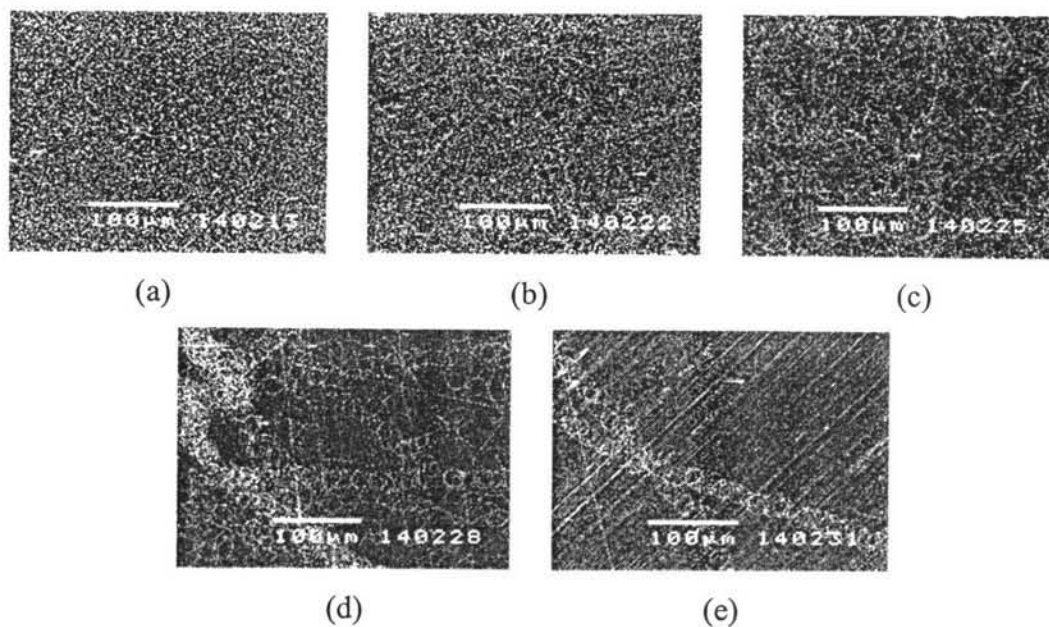


Figure 4.5 Selected SEM images of the as-spun fibers from sonicated 10% (w/v) PVA solutions which were collected from distances of (1) 0, (2) 3, (c) 6, (d) 9, and (e) 12 cm far from the center of deposition area. The applied potential was 15 kV over collection distance of 15 cm. The feed flow rate was 1 ml/hr. Original magnification = 200x and scale bar = 100 μm .

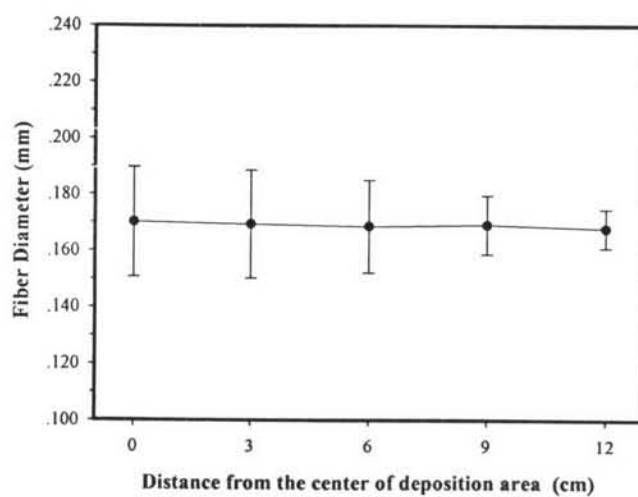


Figure 4.6 Average diameters (μm) of the as-spun fibers from sonicated 10% (w/v) PVA solutions which were collected from various distances far from the center of deposition area. The applied potential was 15 kV over collection distance of 15 cm. The feed flow rate was 1 ml/hr.

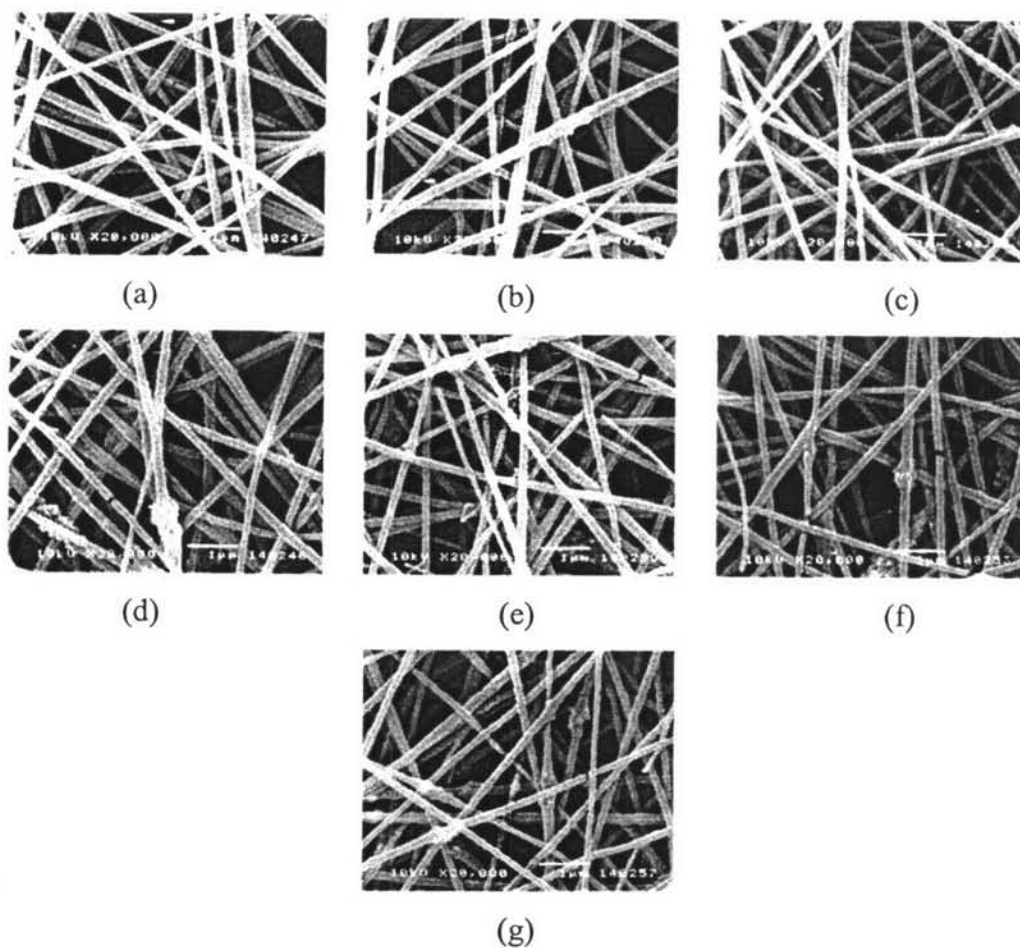
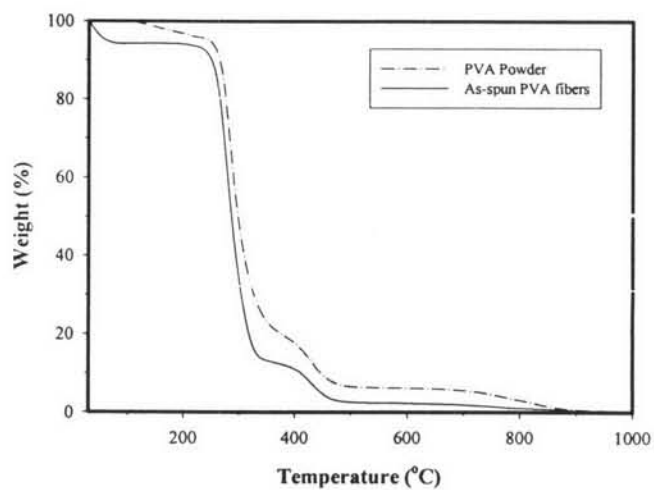
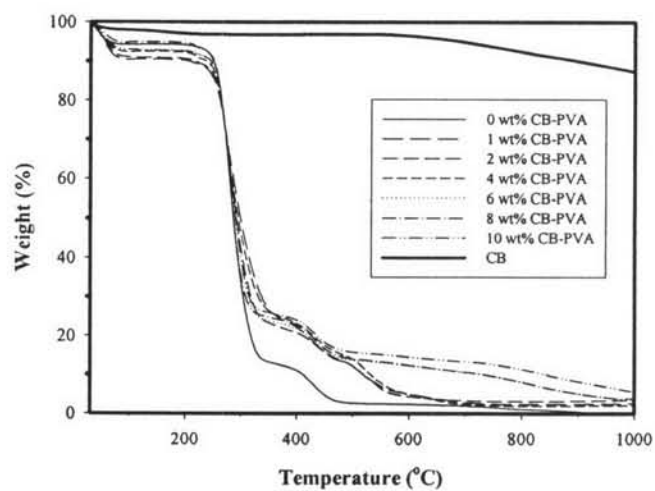


Figure 4.7 Selected SEM images of the as-spun fibers from as-prepared CB-loaded 10% (w/v) PVA solutions at CB contents of (a) 0, (b) 1, (c) 2, (d) 4, (e) 6, (f) 8, and (g) 10 wt% (base on the weight of PVA). The applied potential was 15 kV over collection distance of 15 cm. The feed flow rate was 1 ml/hr. Original magnification = 20kx and scale bar = 1 μm.



(a)



(b)

Figure 4.8 TGA thermograms of (a) PVA powder and as-spun pristine PVA fibers; and (b) CB and as-spun CB-loaded PVA fiber at various content of CB.

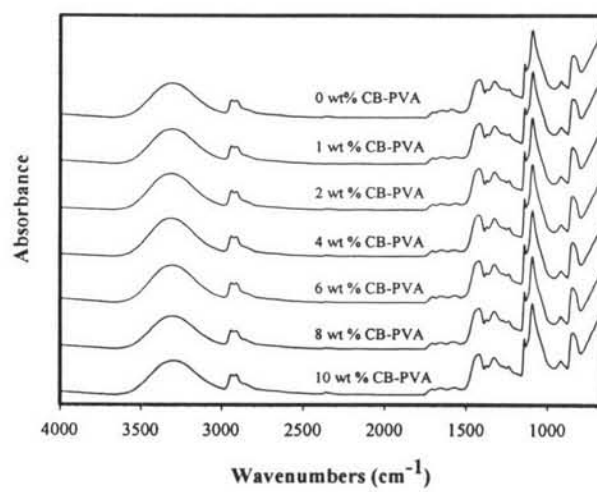


Figure 4.9 IR spectra of as-spun CB-loaded PVA fibers at various CB contents.

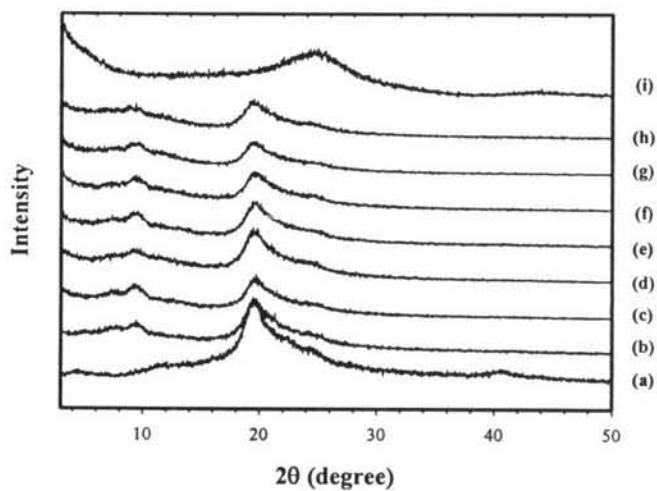
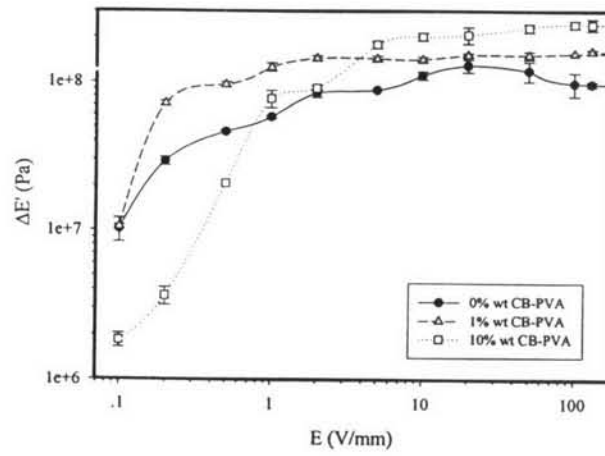
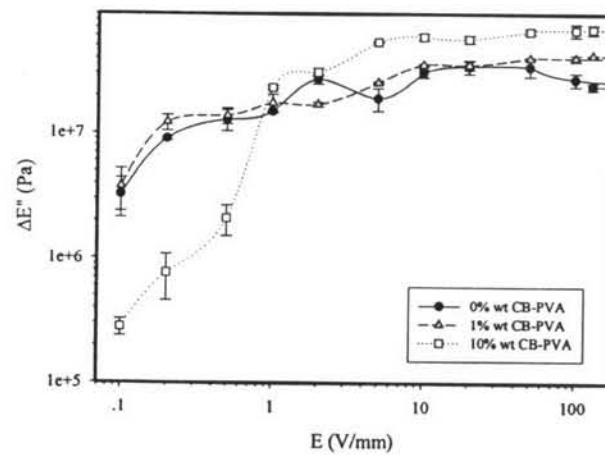


Figure 4.10 WAXD patterns of: (a) PVA powder; (b) as-spun PVA fibers; (c-h) 1, 2, 4, 6, 8, 10 wt% as-spun CB-loaded (base on weight of PVA) PVA fibers, respectively; and (i) CB nanoparticles.

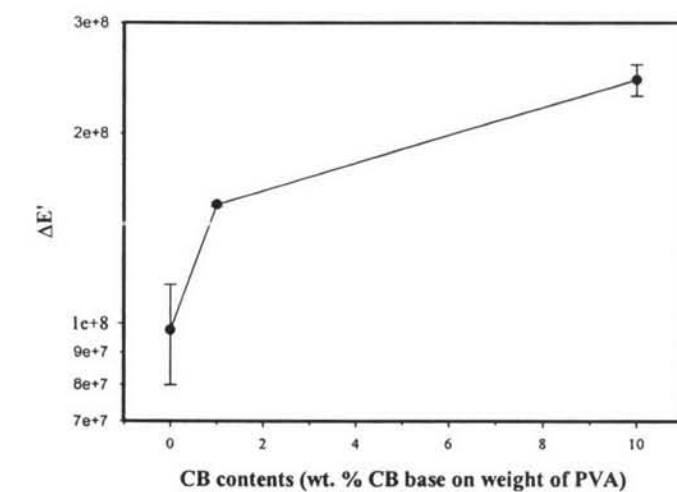


(a)

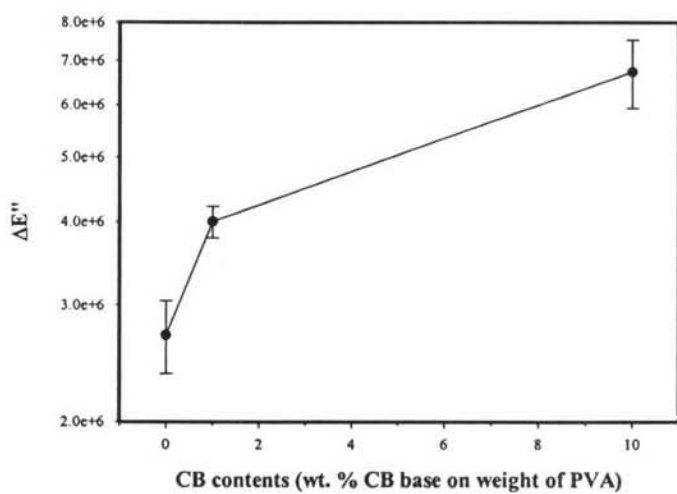


(b)

Figure 4.11 Responses of the modulus of as-spun CB-loaded PVA fibers at various electric field strength and various compositions of CB, frequency = 1.0 rad/s and strain = 0.3 % at 27°C: (a) storage modulus [$\Delta E'(w)$] and (b) loss modulus [$\Delta E''(w)$].



(a)



(b)

Figure 4.12 Responses of the modulus of as-spun CB-loaded PVA fibers at electric field = 100 V/mm: (a) storage modulus [$\Delta E'(w)$] and (b) loss modulus [$\Delta E''(w)$].